

6. A. Simon, R. W. Short, E. A. Williams, and T. Dewandre, *Phys. Fluids* **26**, 3107 (1983).
7. B. B. Afeyan (private communication).
8. W. Seka, E. A. Williams, R. S. Craxton, L. M. Goldman, R. W. Short, and K. Tanaka, *Phys. Fluids* (to be published August, 1984); see also LLE Review **11**, 3 (1982); **17**, 18 (1983).
9. R. E. Turner, D. W. Phillion, B. F. Lasinski, and E. M. Campbell, *Phys. Fluids* **27**, 511 (1984).
10. T. W. Johnston (private communication).
11. H. Figueroa, C. Joshi, H. Azechi, N. A. Ebrahim, and K. Estabrook, *Phys. Fluids* (to be published, 1984).

## 2.C Illumination-Uniformity Considerations for Direct-Drive Fusion Reactors

Several authors have studied the illumination uniformity attainable with overlapped multiple laser beams on a spherical target.<sup>1-4</sup> Skupsky and Lee<sup>5</sup> were the first to decompose the illumination pattern on a sphere in terms of spherical harmonics, in order to analyze the nonuniformity pattern according to its spatial wavelengths. The wavelength information is important because a short-wavelength nonuniformity might be smoothed by thermal conduction within the pellet. Reference 5 includes a nonuniformity analysis of the existing 24-beam OMEGA facility at LLE, as well as a 32-beam, f/20 system. It was shown that the 32-beam system could achieve the required uniformity of less than 1% rms in a limited focal region while occupying only 0.5% of the reactor solid angle. Modest thermal smoothing extended the useful region of the 32-beam geometry to include the entire focal region of interest for direct-drive laser fusion. We have extended the work in Ref. 5 to include 20, 32, 60, and 96 beams evaluated for 2% and 8% solid-angle fractions in the reactor. This activity is part of a preconceptual reactor design named SIRIUS conducted in collaboration with the Nuclear Engineering Department of the University of Wisconsin.<sup>6</sup>

The disposition of the final optical elements in the reactor chamber is determined by three related variables: (1) the size of the laser aperture, (2) the distance from the target, and (3) the solid angle subtended by the beams. The laser aperture is determined by the total laser energy and the laser-induced damage threshold of the last focusing optic. The final optic spacing from the pellet determines the reaction-product loading on the optic, and the solid-angle fraction has an impact on the performance of the reactor-blanket. Any two of these variables determine the third. We have chosen to estimate both the laser aperture and an acceptable total solid angle, thereby fixing the final optic distance without regard to the reaction-product loading. It should be noted that holding the solid-angle fraction constant as

the number of beams, N, is varied does not change the distance of the final optic from the pellet. This allows us to study the illumination uniformity effects of N beams without changing this basic design parameter.

The total aperture of the laser driver is determined by the laser energy and the optical damage threshold of the reflective coating on the last focusing optic. For this study we have used values of 2 mJ for the driver energy (at 248 nm) and a damage threshold of 5.0 J/cm<sup>2</sup>. When the damage threshold value is combined with the assumed geometrical fill factor (0.7) and a safety factor for ripples on the beam (0.5), the overall threshold is 1.75 J/cm<sup>2</sup>. This dictates a total laser aperture of 144 m<sup>2</sup>. This aperture is independent of the system configuration, whether direct or indirect drive. The corresponding single-beam apertures for 20, 32, 60, and 96 beams are given in Table 19.I.

NUMBER OF BEAMS	20	32	60	96
beam aperture (m)	2.7	2.1	1.6	1.2
f-number for 2% solid angle fraction	7.9	10.0	13.7	17.3
f-number for 8% solid angle fraction	3.9	5.0	6.8	8.6

- Final optic spacing from pellet  
 2% solid angle fraction - 21.3 m  
 8% solid angle fraction - 10.6 m

A105

Table 19.I  
 SIRIUS parameters.

The second variable in the system configuration is the solid-angle fraction the driver occupies in the reactor. This is related to the number of beams and the f-number of the beams by the following expression:

$$\frac{\Delta\Omega}{4\pi} = \frac{N}{2} \left( 1 - \frac{2f}{(4f^2+1)^{1/2}} \right) \tag{1}$$

For the SIRIUS study we are evaluating 2% and 8% solid-angle fractions for the laser beams. The appropriate f-numbers for each of the beam configurations has been calculated using Eq. 1 and is given in Table 19.I. This f-number and the individual beam aperture give the spacing of the final optic from the pellet. The 2% solid-angle fraction places the final optic 21.3 m from the pellet, and the 8% solid-angle fraction has a 10.6-m spacing. This approach allows an evaluation of the effect of dividing the total laser aperture into N beams while maintaining a constant solid-angle fraction in the reactor. The cost scaling of the driver with N is not currently well understood and is beyond the scope of this study. Here we attempt to show the uniformity scaling with N, so that future work can balance the cost scaling of a driver against the uniformity scaling.

The formalism used in this work has been described in detail in Ref. 5 and is briefly reviewed here. The irradiation pattern on the sphere is decomposed into spherical harmonics where the standard deviation of a mode amplitude is given by

$$\sigma_l = \left| \frac{E_l}{E_0} \right| \left[ (2l+1) \sum_{k,k'} P_l(\Omega_k \cdot \Omega_{k'}) \frac{W_k W_{k'}}{W_T^2} \right]^{1/2} \quad (2)$$

The single-beam factor  $|E_l/E_0|$  is determined by the focus position, f-number, beam profile, and assumed target conditions. This single-beam factor is evaluated by tracing rays through the pellet plasma shown in Figure 19.11. The remainder of Eq. 2 is the geometrical factor which is determined by the number and orientation of the beams ( $\Omega_k$ ) and the beam energies ( $W_k$ ). The sum is over all beams;  $W_T = \sum W_k$  and  $P_l$  is a Legendre polynomial. The rms standard deviation of all modes is defined as

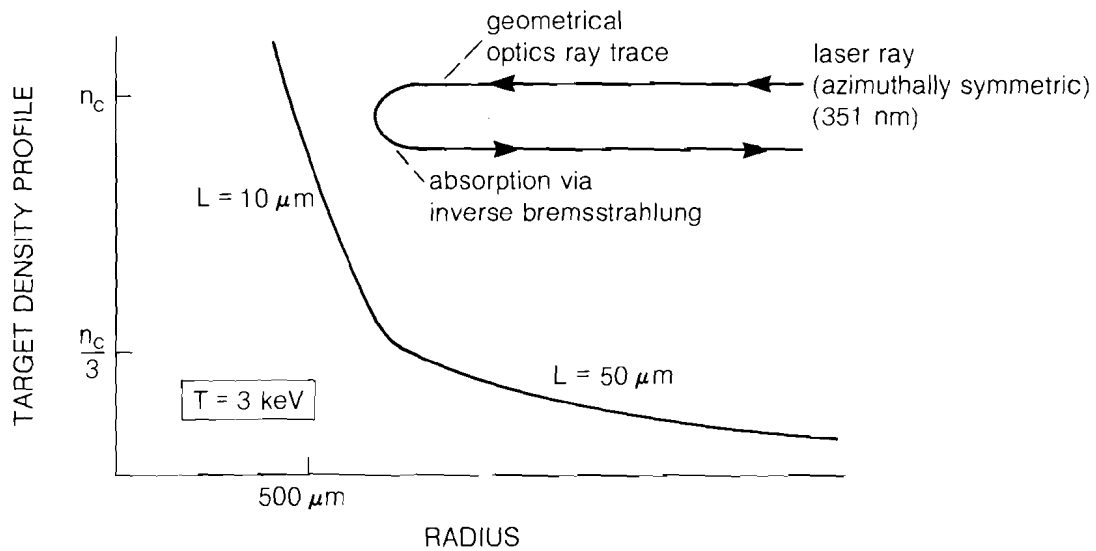
$$\sigma_{rms} = \left( \sum_{l \neq 0} \sigma_l^2 \right)^{1/2}. \quad (3)$$

We have calculated the nonuniformity, in terms of  $\sigma_{rms}$ , for a variety of conditions. Earlier work<sup>5</sup> indicated that a quadratic beam-intensity profile of the following form produced good uniformity

$$I = I_0 \left( 1 - \frac{r^2}{r_0^2} \right) \quad (4)$$

Fig. 19.11  
Target conditions for single-beam factor calculations.

where  $r_0$  is the pellet radius.



A95

The  $\sigma_{rms}$  for a 2% solid-angle fraction geometry is plotted in Fig. 19.12 for 20, 32, 60, and 96 beams as a function of a focus ratio. The focus ratio is defined as

$$\text{focus ratio} = \frac{F}{2fr_0} \quad (5)$$

F is the position (in mm) of the geometrical best focus beyond the pellet center,  $r_0$  is the pellet radius (in mm), and f is the beam f-number. A focus ratio of 1 corresponds to tangential focus where the beam aperture ( $2R_0$ ) illuminates a hemisphere of the pellet ( $2r_0$ ).

The maximum tolerable nonuniformity is generally assumed to be around 1% rms for targets with a convergence ratio (ratio of initial to compressed fuel radius) of less than  $\sim 20$ . Such uniformity must be maintained during the entire time of laser irradiation. Figure 19.12 shows that rms nonuniformities of less than 1% can be achieved over a specific range of focus ratios. The focus ratio changes during the implosion as the target is compressed [i.e.,  $r_0$  in Eq. (5) becomes smaller]. Reactor target simulations indicate that the target can be driven to  $\sim 60\%$  of its initial radius by the time that the laser pulse attains maximum intensity. Therefore, if the initial focus is tangential, that is, focus ratio = 1, then the focus ratio will increase during target compression to a value of 1.67 at peak pulse intensity. To obtain high uniformity over this range, Fig. 19.12 shows that one option for direct-drive laser fusion is to use 60 or more beams.

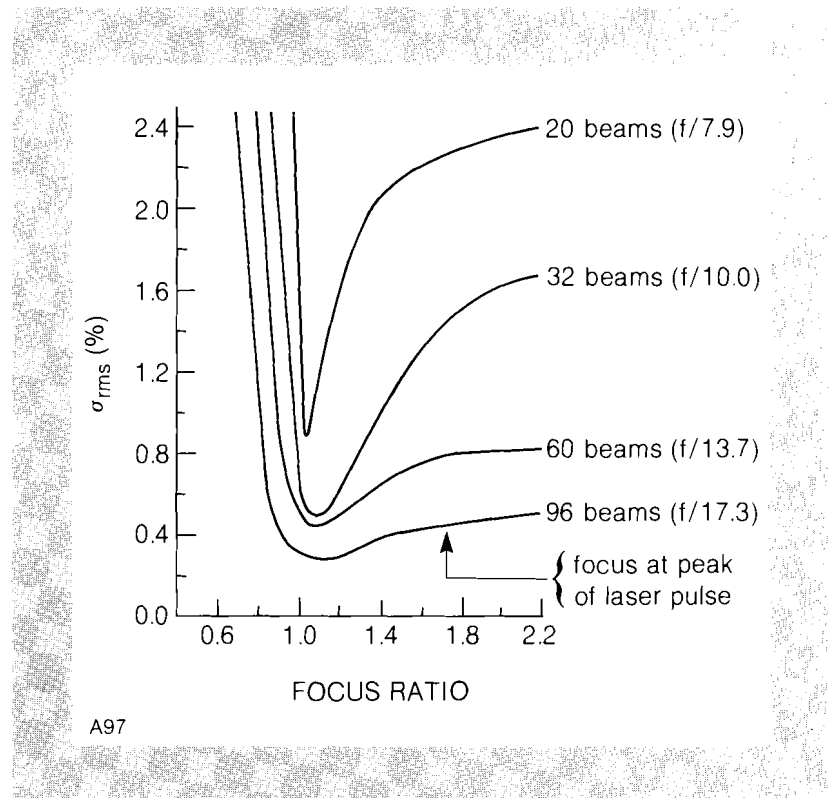


Fig. 19.12  
Nonuniformity of laser-energy deposition  
for 2% solid-angle fraction.

High drive uniformity can also be obtained with few beams ( $\sim 32$ ) if thermal smoothing within the target is found to be effective. This is illustrated in Fig. 19.13 for a 32-beam system at  $f/20$ . The dotted curve represents the attenuation of nonuniformities due to moderate thermal smoothing and shows that less than 0.5% rms nonuniformity is maintained over the entire focal region of interest. For this calculation it was assumed that the fractional separation distance between the critical and ablation surfaces ( $\Delta R/R$ ) was 0.1, which is characteristic of short-wavelength laser irradiation during the time of significant laser-energy deposition.

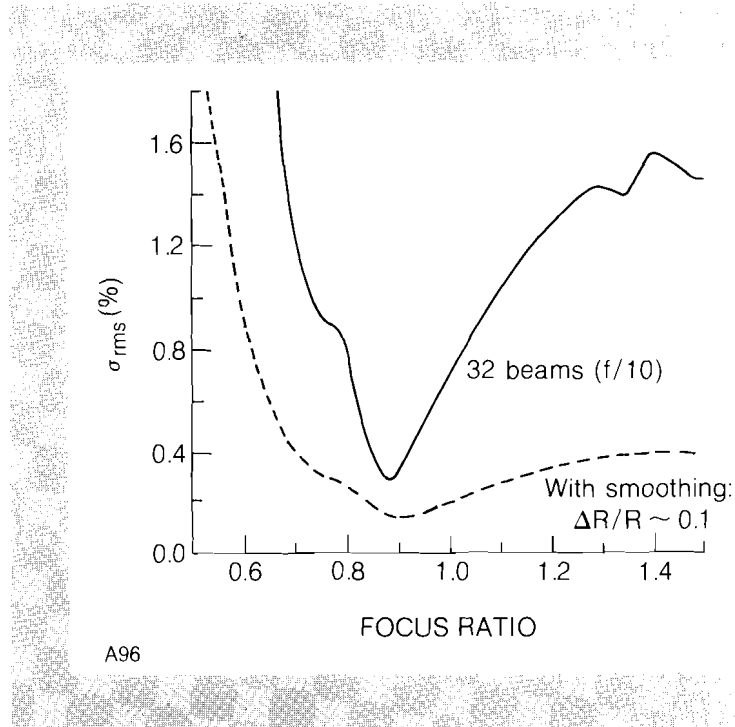
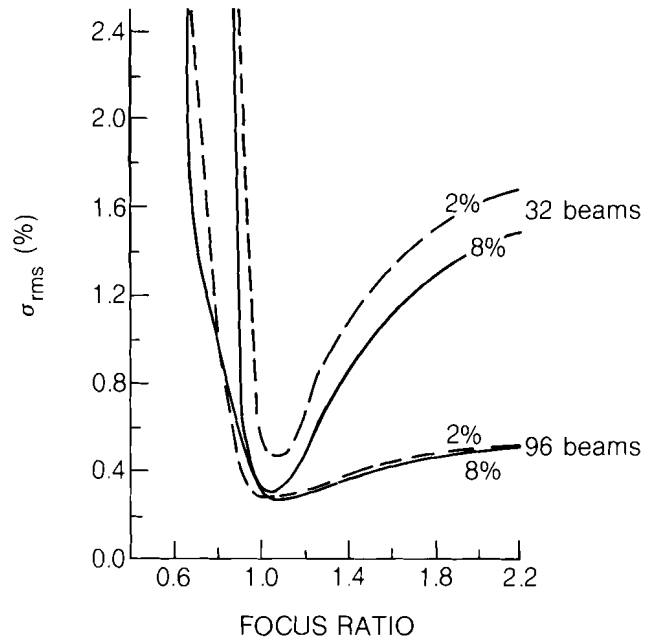


Fig. 19.13  
The effect of moderate thermal smoothing on the 32-beam nonuniformity.

The effect of changing the total solid angle subtended by the beams has been studied and is displayed in Fig. 19.14. There is a small improvement in uniformity for the 32-beam system in going from 2% to 8% of  $4\pi$ , resulting from the change between  $f/10$  and  $f/5$  optics. Changes above  $\sim f/10$  have a negligible effect on uniformity as seen in the 96-beam case which represents a change from  $f/9$  to  $f/17$ , because the laser rays are already effectively parallel.

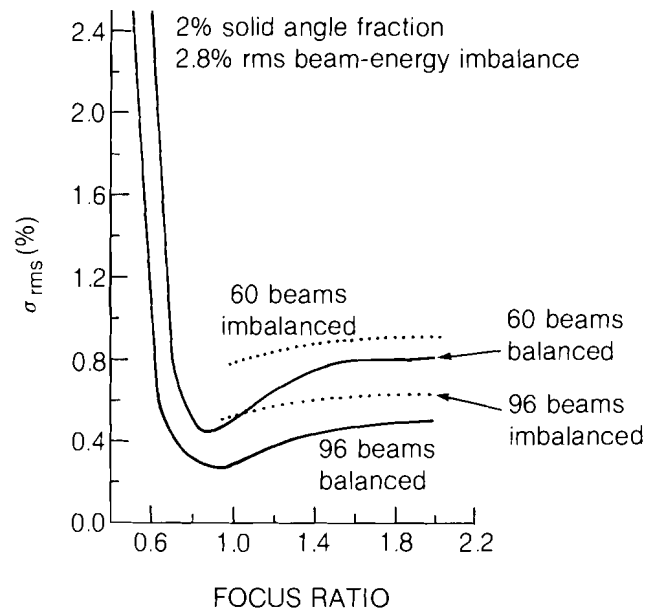
The effects of beam-to-beam energy imbalance were also studied. These create predominantly long-wavelength nonuniformities ( $l \leq 4$ ). The sensitivity to energy imbalance is reduced as the number of beams is increased. Figure 19.15 shows the effect of a 2.8% rms random variation for the 60- and 96-beam geometries. With this imbalance, typical of the value achieved on OMEGA, the irradiation nonuniformity still stayed below 1% rms.

These calculations used an idealized laser-beam profile. Realistic radial-beam profiles might not be as smooth as the quadratic form used here due to, for example, diffraction effects. The effect of small-



A100

Fig. 19.14  
Uniformity for increased solid-angle fraction.



A101

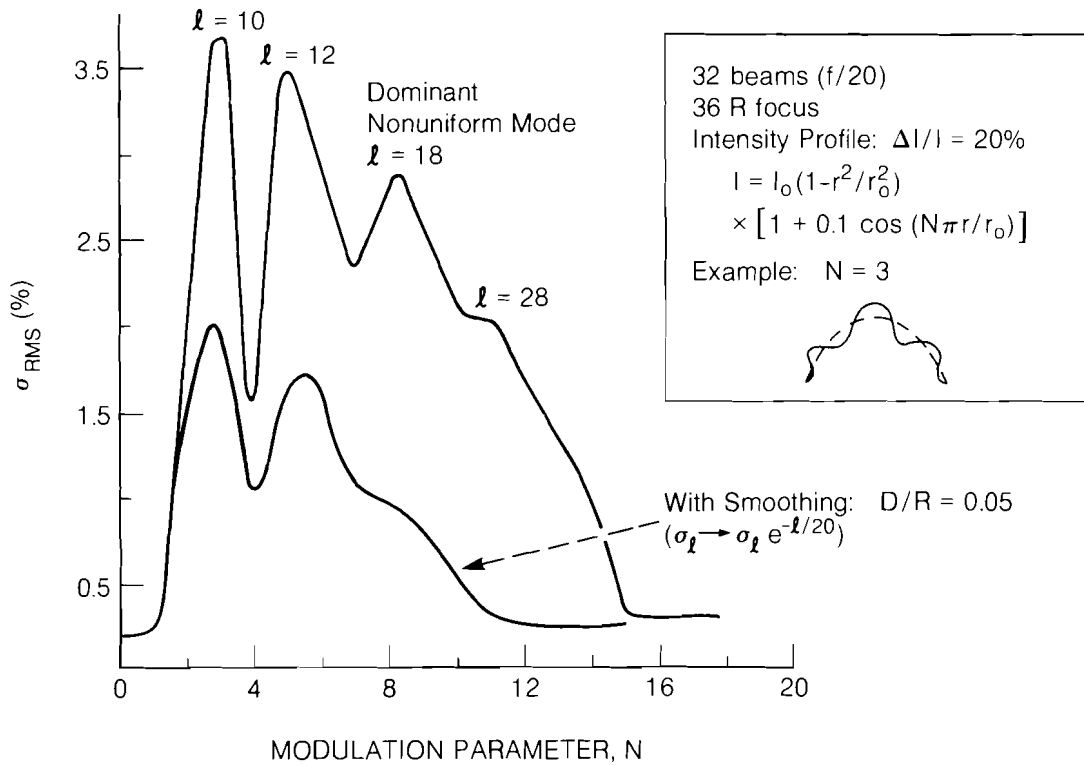
Fig. 19.15  
Uniformity with energy imbalance.

scale variations on the radial-beam shape has been examined using a modulated quadratic profile of the form:

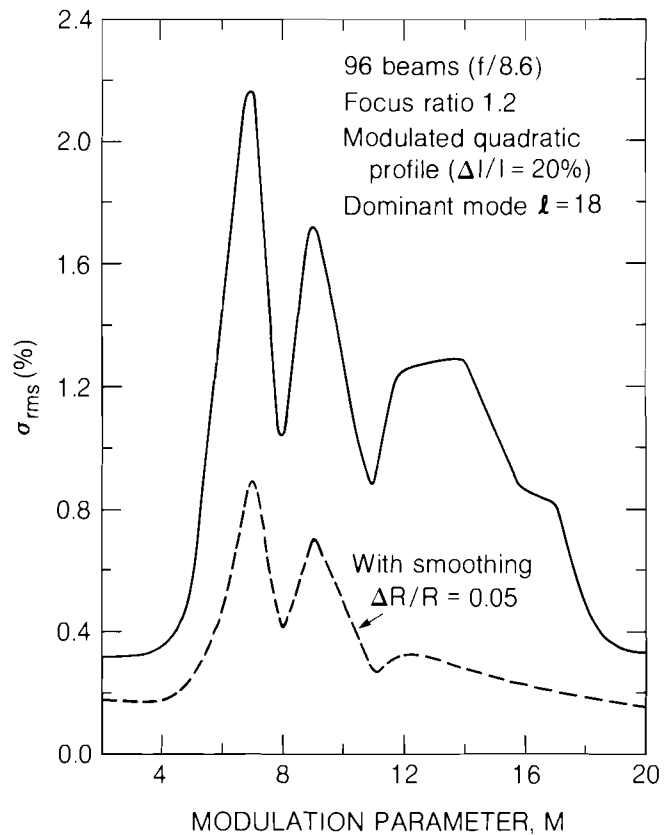
$$I = I_0 \left(1 - \frac{r^2}{r_0^2}\right) [1 + \epsilon \cos(\pi M r / r_0)]$$

where  $\epsilon$  and  $M$  are parameters controlling the magnitude and wavelength of the modulations. Physically,  $M/2$  can correspond to the number of diffraction rings. Figures 19.16 and 19.17 are nonuniformity calculations for 32 and 96 beams with a 2% solid-angle fraction. To demonstrate the effect of only a small amount of smoothing, we multiply each  $\sigma_l$  by the factor  $\exp(-l/20)$ , corresponding to  $\Delta R/R = 0.05$ . Note the rapid drop in nonuniformity for  $M > 8$ . Additional simulations have shown the magnitude of the nonuniformities scales approximately linearly with  $\epsilon$ . These results suggest that laser systems for future fusion reactors should be designed with not less than  $\sim 4$  diffraction rings and/or an intensity variation  $\Delta I/I$  considerably less than the 20% used here, both of which are within the limits of present-day technology (see Fig. 19.18). In addition, the effect of the intensity modulation is greatly reduced as the number of beams is increased.

Fig. 19.16  
32-beam modulated profile.



TC1399

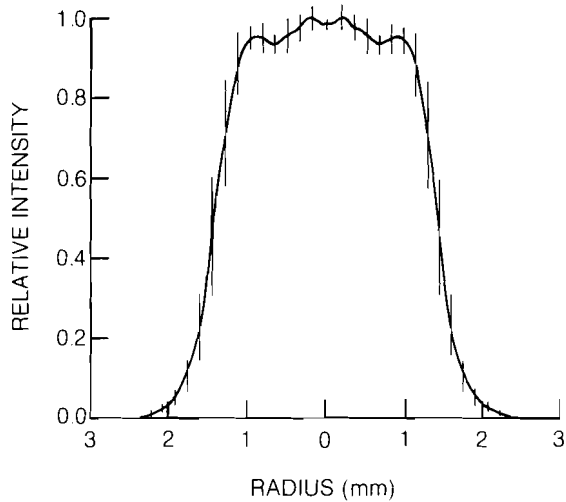


A107

Fig. 19.17  
96-beam modulated profile.

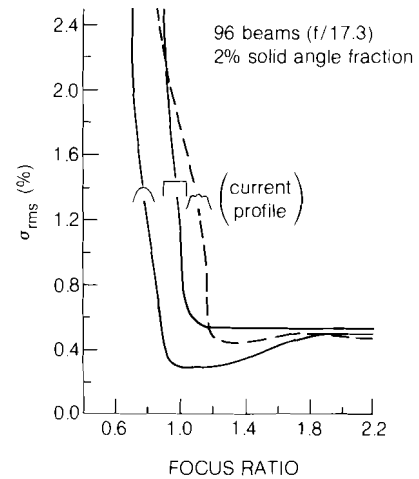
We routinely measure the intensity distribution of LLE lasers at the plane of the target. These photographs are referred to as equivalent-target-plane or ETP photos. Generally these are digitized, and an azimuthally averaged plot is generated. One such plot is shown in Figure 19.18. This profile was compared with the quadratic and flat-top profiles for a 96-beam geometry in Figure 19.19. This current profile approaches both idealized profiles if the focus ratio is around 2.0, because the central portions of all three profiles are similar.

The extension of the spherical harmonic analysis of symmetric illumination to 96 beams has shown that the sensitivity of the pellet illumination uniformity to various perturbations, such as energy imbalance and intensity modulation, is greatly diminished when a large number of beams are used. Using greater than  $\sim 60$  beams (with the total beam solid angle at  $\sim 2\%$ ) provides one possible option for the direct-drive approach to laser fusion. If thermal smoothing is found to be an effective mechanism for reducing nonuniformities, then fewer beams, around 32, could provide adequate illumination uniformity.



TC1409

Fig. 19.18  
Current beam profile from LLE laser system.



A98

Fig. 19.19  
Uniformity depends on laser beam profile.

#### ACKNOWLEDGMENT

This work was supported by the U.S. Department of Energy Office of Inertial Fusion under contract number DE-AC08-80DP40124 and by the Laser Fusion Feasibility Project at the Laboratory for Laser Energetics which has the following sponsors: Empire State Electric Energy Research Corporation, General Electric Company, New York State Energy Research and Development Authority, Northeast Utilities Service Company, Southern California Edison Company, The Standard Oil Company, and University of Rochester. Such support does not imply endorsement of the content by any of the above parties.

#### REFERENCES

1. J. E. Howard, "Uniformity of Illumination of Spherical Laser-Fusion Targets," *Appl. Opt.* **16**, 2764 (1977).
2. J. B. Trenholme, "Target Illumination of Shiva," Laser Program Annual Report - 1974, LLNL Report UCRL-50021-74, Livermore, CA.
3. J. B. Trenholme and E. J. Goodwin, "Theory and Design Analysis," Laser Program Annual Report - 1979, LLNL Report UCRL-50021-79, Livermore, CA.
4. J. B. Trenholme, "Nova Target Illumination Studies," Laser Program Annual Report - 1980, LLNL Report UCRL-50021-80, Livermore, CA.
5. S. Skupsky and K. Lee, *J. Appl. Phys.* **54**, 3662 (1983).
6. "Preliminary Conceptual Design of SIRIUS, A Symmetric Illumination, Direct Drive Laser-Fusion Reactor," University of Wisconsin Report UWFD-568 and LLE Report 152.
7. S. E. Bodner, *J. Fusion Energy* **1**, 221 (1981).
8. R. Kingslake, *Lens Design Fundamentals* (Academic Press, 1978).
9. Copyright by Genesee Computer Center Inc., Rochester, New York.